Charge transfer in photovoltaics consisting of interpenetrating networks of conjugated polymer and TiO$_2$ nanoparticles

A. C. Arango and S. A. Carter[a)]
Physics Department, University of California, Santa Cruz, California 95065

P. J. Brock
IBM Almaden Research Center, San Jose, California 95120

We study the effect of blended and layered titanium dioxide (TiO$_2$) nanoparticles on charge transfer processes in conjugated polymer photovoltaics. A two order of magnitude increase in photoconductivity and sharp saturation is observed for layered versus blended structures, independent of the cathode work function. Using electrodes with similar work functions, we observe low dark currents and open circuit voltages of 0.7 V when a TiO$_2$ nanoparticle layer is self-assembled onto the indium–tin–oxide electrode. Our results for the layered morphologies are consistent with charge collection by exciton diffusion and dissociation at the TiO$_2$ interface. © *1999 American Institute of Physics.* [S0003-6951(99)00212-0]

Over the last decade, soluble conjugated polymers have become attractive for use as inexpensive large area photodetectors and solar cells. Although polymer photoconductivities are severely limited by low charge mobilities, short exciton diffusion lengths, and low absorption,[1,2] recent work has shown that the use of interpenetrating donor-acceptor heterojunctions, such as polymer/C60 nanoparticle composites,[3,4] polymer/CdSe nanoparticle composites[5] and interpenetrating polymer networks[6] can substantially improve the photoconductivity, and thus quantum efficiency, of polymer-based photovoltaics. In these devices, an exciton is photogenerated in the active material, diffuses towards the donor–acceptor interface, and dissociates via charge transfer across the interface. The internal electric field set by the difference between the electrode energy levels, and the donor-acceptor morphology control the quantum efficiency of the cell. An alternative approach to efficient large area photovoltaics was introduced by O'Regan and Grätzel in 1990 using porous dye-sensitized TiO$_2$ nanocrystalline layers to form efficient electrochemical solar cells.[7] In these devices, the high power efficiencies (10%) are attributable to the ultrafast charge transfer from the dye to the TiO$_2$, the high surface area of the TiO$_2$ film, the broad absorption of the dye, and the efficient separation of opposite charge into different materials. Here, the quantum efficiency and internal electric field are dependent on the relative energy levels and bonding properties of the photoconducting dye and the porous TiO$_2$ nanoparticle surface.[8–10]

In this letter, we study the effect of polymer/nanoparticle morphology on the device properties of organic thin film photovoltaics by incorporating either individual TiO$_2$ nanoparticles or a porous nanocrystalline TiO$_2$ layer into which the polymer penetrates. In forward bias, a two order of magnitude increase in photoconductivity, along with sharp photocurrent saturation, is observed in the layered structures in contrast to blends where no enhancement occurs. When a self-assembled monolayer is incorporated into the layered device, we observe low forward-bias dark currents and open

circuit voltages that are determined by the conducting band energy of the TiO$_2$.

We use poly(2-methoxy-5(2-ethyl)hexoxy-phenylene-vinylene (MEH-PPV), as both the active photogeneration medium and the hole transporter. Fabrication of the polymer/TiO$_2$ nanoparticle blend has been described previously.[11] Sintered nanocrystalline TiO$_2$ layers are made by coating an indium–tin–oxide (ITO) patterned glass substrate with a viscous TiO$_2$ water solution that is spread onto the substrate and annealed for 30 min at 500 °C to fuse the nanoparticles. The opaque TiO$_2$ layers are typically 4–6-μm-thick and strongly adhere to the substrate. An atomic force microscope (AFM) image of the surface of a micron thick TiO$_2$ film reveals an average particle size of 80 nm with estimated pore diameters above 20 nm, near the exciton diffusion length in MEH-PPV.[10] The sample is transferred into a nitrogen glove box where a thin layer of MEH-PPV is spun onto the TiO$_2$ layer. As the polymer penetrates into the pores, the opaque TiO$_2$ layer becomes transparent. A monolayer of TiO$_2$ is self-assembled onto the ITO surface using activation of the ITO surface with 3-aminopropyltriethoxysilane. Current–voltage (I–V) characteristics are measured with a Keithley 2400 source-measure unit in a nitrogen atmosphere under illumination through the ITO side by a halogen source with an intensity of 2 mW/cm$_2$ over the absorption region of the polymer. Photocurrent action spectra are taken with a Halogen lamp, a chopper, a monochromator, and a lock-in amplifier.

Current–voltage characteristics in dark and under illumination of a TiO$_2$ composite device and a TiO$_2$ layered device are compared in Fig. 1. Both devices are sandwiched between ITO and calcium. In the dark, the I–V curve for the blended device is similar in form and magnitude to those for devices of lower nanoparticle concentrations reported earlier; these devices have enhanced electroluminescence under forward bias.[10] Under illumination, we observe a slightly larger photoconductivity than for pure MEH-PPV devices. In contrast, current flow through the layered device in the dark under forward bias is near the noise level of the instrumentation and only a small amount of current flow is observed in
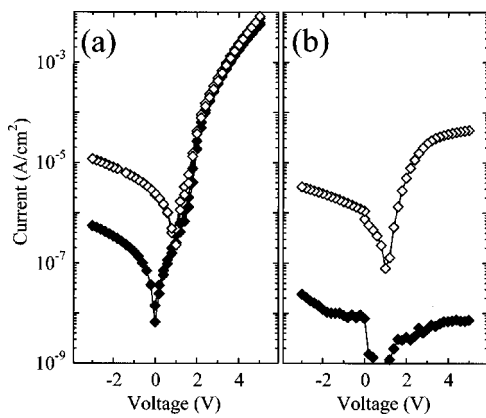
[a)]Electronic mail: sacarter@cats.ucsc.edu

FIG. 1. The current–voltage curves in light (open diamonds) and in the dark (closed diamonds) for polymer/TiO$_2$ photocells for (a) blended structures (70% by weight of TiO$_2$ to polymer) and (b) layered structures are plotted on a logarithmic scale. The TiO$_2$ layer serves as an electron acceptor and a hole blocking layer. Calcium and ITO serve as the cathode and anode, respectively.
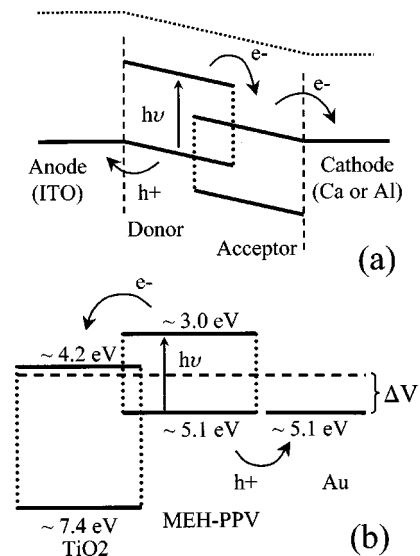

FIG. 2. Energy diagrams depicting the transfer of charge for the (a) traditional donor-acceptor model and (b) the Grätzel-like model. In traditional donor-acceptor photocells, the open circuit voltage is mainly due to the difference in work functions between the anode (ITO) and the cathode (Ca or Au) because the polymer layer is insulating at low voltages. In Grätzel cells, the anode and the cathode serve only as quasi-ohmic contacts and the maximum open circuit voltage is determined by the difference between the Fermi level of the TiO$_2$ under illumination and the HOMO of the replenishing species.

reverse bias. In light, the $I-V$ curve of the layered device retains essentially the same rectified form as that of the composite device; however, the electroluminescence is quenched and the current saturates above 4 V. The open circuit voltages are typically 1.0 V for both blended and layered devices.

The inability of the TiO$_2$ nanoparticles to quench electroluminescence in the polymer suggests that the isolation of individual nanoparticles within the polymer limits the occurrence of charge transfer. As shown in Fig. 2(b), the alignment of energy levels at the TiO$_2$/MEH-PPV interface is such that an electron in the polymer may lower its energy by charge transfer to a TiO$_2$ nanoparticle. Nanoparticle isolation within the polymer matrix, however, can prevent significant charge transfer because electron transfer from the MEH-PPV to the isolated nanoparticles would result in charge buildup on a single site, impeding further charge transfer from the MEH-PPV.[12] Therefore, nonpercolating aggregation of the TiO$_2$ nanoparticles inhibits the formation of an internal network of donor-acceptor heterojunctions, as required for sustained charge transfer from the polymer to the TiO$_2$.

Characterization of the TiO$_2$ layered device $I-V$ curves is facilitated by consideration of the energy band diagram (neglecting band bending or other surface effects) to illustrate the charge transfer processes that occur during current flow. For the flow of current through the cell in the dark in forward bias, three essential charge transfer processes are required: (1) electron injection from the Ca electrode to the conduction band of MEH-PPV, (2) hole injection from the ITO electrode to the valence band of the TiO$_2$, and (3) hole transfer from the TiO$_2$ to the valence band of the MEH-PPV. Both the second and third charge transfer processes are unlikely because of the relative energy levels and insulating nature of the TiO$_2$ layer, resulting in the absence of current flow in the dark state. We consider electron flow through the device to be negligible due to the presence of electron traps. Current flow under illumination in forward bias requires that an exciton generated in the MEH-PPV layer transfer negative charge to the conduction band of the TiO$_2$ and transfer positive charge to the Ca electrode. The electron must also continue to flow out of the TiO$_2$ to the ITO elec-

trode. Since all of the above charge transfer processes are energetically favorable, current may flow through the diode under illumination due to the ability of the TiO$_2$ layer to accept and conduct photoexcited electrons.

The role of the TiO$_2$ layer is further illustrated by using symmetric contacts, namely Au and ITO, with work function of $5.1+0.1$ and $4.8+0.2$,[13] respectively. We show the current–voltage characteristics for such a device using the same sintered TiO$_2$ layer discussed before [Fig. 3(a)] and for a device where a self-assembled TiO$_2$ monolayer has been incorporated into the device structure [Fig. 3(b)]. When the self-assembled TiO$_2$ monolayer is included, the open circuit voltage increases to -0.7 V. The monolayer also results in a substantial decrease in the dark current in forward bias. All
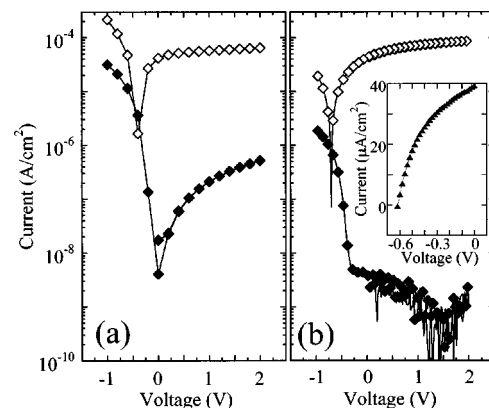

FIG. 3. The current–voltage curves in light (open diamonds) and in the dark (closed diamonds) for layered polymer/TiO$_2$ photocells (a) without and (b) with a self-assembled TiO$_2$ monolayer at the ITO surface are plotted on a logarithmic scale. The inset shows a linear current–voltage plot of the monolayer device under illumination revealing a fill factor of 0.43. Symmetric contacts are provided by the gold and ITO electrodes, which serve as the cathode and anode, respectively.
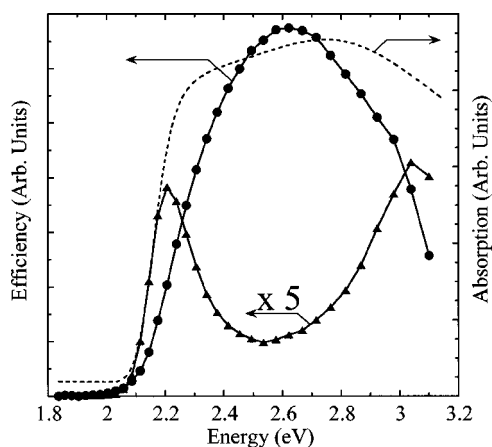
FIG. 4. The photocurrent action spectrum for the ITO/TiO$_2$/MEH-PPV/Au photocell (circles) as compared with an ordinary ITO/MEH-PPV/Ca diode (triangles). The absorption of MEH-PPV (dotted line) corresponds with the photocurrent spectrum of the layered device (symbatic response), which is due to reversal of the internal field and dissociation at the polymer/TiO$_2$ interface.

layered devices show a similar sharp saturation in photocurrent in forward bias, which implies that exciton diffusion and dissociation at the TiO$_2$ interface is the dominant process for the collection of charge. According to the traditional donor-acceptor model, the internal electric field is mainly due to the asymmetry between the electrode work functions [Fig. 2(a)]. This model, as applied to our ITO/TiO$_2$/MEH-PPV/Au device, may account for the negative open circuit voltages, but fails to account for the magnitude (0.7 V) observed for the nearly symmetric Au and ITO contacts. However, a model analogous to that employed by O'Regan and Grätzel [shown in Fig. 2(a)], which neglects the ITO electrode altogether and treats the TiO$_2$ layer as the front electrode, coincides more accurately with the observed open circuit voltages for the self-assembled monolayer device. In this case, the internal field is the difference between the ''quasi-Fermi level'' of the TiO$_2$ under illumination (-4.2 eV), and the work function of the MEH-PPV highest occupied molecular orbital (HOMO) and/or gold electrode (-5.1 eV). Thus, the rectified form and the open circuit voltages of the I–V characteristic of the ITO/TiO$_2$/MEH-PPV/Au device can be explained by assuming exciton generation in the polymer, exciton diffusion to the TiO$_2$ interface, exciton dissociation at the interface, collection by diffusion of holes, and electrons to the gold cathode and ITO anode, respectively. Such behavior is expected whenever direct contact between the ITO and MEH-PPV is suppressed, as is the case for the TiO$_2$ self-assembled devices.

Comparison in Fig. 4 of the zero-bias photocurrent action spectrum of a pure MEH-PPV device sandwiched between ITO and Ca with a TiO$_2$ layered device identifies a significant advantage realized by the TiO$_2$ electrode. The maximum response of the pure device does not correlate with maximum absorption of the polymer (antibatic) while the response of the TiO$_2$ electrode device matches the absorption (symbatic) and, thus, broadens the region of light sensitivity of the cell. Since the TiO$_2$ layer reverses the direction of the internal field, the internal filter effect that is often observed in pure devices is avoided.[14] Unlike pure devices, where light must traverse a significant amount of the

bulk polymer before reaching the active region where charge generation occurs, in TiO$_2$ electrode devices, light passes through the transparent TiO$_2$ layer to the polymer/semiconductor interface where the majority of charge is believed to be produced. We find that device sensitivity to low levels of illumination is reduced, which may imply that the polymer/semiconductor interface is less established near the ITO contact due to insufficient penetration of the polymer into the pores of the TiO$_2$ electrode. This effect may explain the quantum efficiencies under 4%. The ability to control pore size, thickness and interfacial surface area should result in higher quantum and power efficiencies.

In summary, we have shown that efficient charge transfer occurs at the MEH-PPV/TiO$_2$ interface, resulting in a device that acts as a solid state nonelectrochemical version of the dye-sensitized Grätzel cell. Because the energy level of the conduction band of the TiO$_2$ semiconductor is low, large open circuit and low saturation voltages can be achieved using stable high work-function electrodes, allowing for flexibility in improving device efficiency, cost, and stability. Furthermore, given the large photoconduction quantum efficiencies that have already been attained in polymer composite photovoltaics,[3–6] stable large-area efficient polymer-based photocells should be achievable in conjugate polymer/TiO$_2$ composite systems through further improvements in the morphology of the TiO$_2$ layer and the penetration of the polymer into the network.

[1] S. Barth, H. Bässler, H. Rost, and H. H. Hörhold, Phys. Rev. B **56**, 3844 (1997).
[2] D. Moses, J. Wang, G. Yu, and A. J. Heeger, Phys. Rev. Lett. **80**, 2685 (1998).
[3] G. Yu, J. Gao, J. C. Hummelen, F. Wudl, and A. J. Heeger, Science **270**, 1789 (1995); G. Yu and A. J. Heeger, J. Appl. Phys. **78**, 4510 (1995).
[4] C. J. Brabec, V. Dyakonov, N. S. Sariciftci, W. Graupner, G. Leising, and J. C. Hummelen, J. Chem. Phys. **109**, 1185 (1998).
[5] N. C. Greenham, X. Peng, and A. P. Alivisatos, Phys. Rev. B **54**, 17628 (1996).
[6] J. J. M. Halls, C. A. Walsh, N. C. Greenham, E. A. Marseglia, R. H. Friend, S. C. Moratti, and A. B. Holmes, Nature (London) **376**, 498 (1995).
[7] B. O'Regan and M. Grätzel, Nature (London) **353**, 737 (1991).
[8] F. Cao, G. Oskam, and P. Searson, J. Phys. Chem. **99**, 17071 (1995).
[9] M. Kocher, T. K. Däubler, E. Harth, U. Scherf, A. Gügel, and D. Neher, Appl. Phys. Lett. **72**, 650 (1998).
[10] T. J. Savenije, J. M. Warman, and A. Goossens, Chem. Phys. Lett. **287**, 148 (1998).
[11] S. A. Carter, J. C. Scott, and P. J. Brock, Appl. Phys. Lett. **71**, 1145 (1997).
[12] L. Bozano, S. Tuttle, S. A. Carter, and P. J. Brock, Appl. Phys. Lett. **73**, 3911 (1998).
[13] J. Holzl and F. K. Schelte, in *Springer Tracts in Modern Physics*, Vol. 85, Solid Surface Physics (Springer, Berlin, 1979), 1–ISO.
[14] M. J. Harrison, J. Gruner, and G. C. W. Spencer, Phys. Rev. B **55**, 7831 (1997).